

Investigations on the CoAPO-36 molecular sieve

Deepak Bansilal Akolekar

*Department of Physical Chemistry, The University of New South Wales, PO Box 1,
Kensington, NSW 2033, Australia*

Received 30 August 1993; accepted 9 July 1994

Highly crystalline cobalt aluminophosphates of type 36 have been synthesized and characterized. Investigations on the thermal decomposition of $\text{Pr}_3\text{N-CoAPO-36}$ and the surface, sorption, acid strength distribution, acidic and catalytic properties of CoAPO-36 were carried out. The XPS analysis indicated that the concentration of cobalt was higher in the bulk of the material than on the surface. The surface of the cobalt aluminophosphate is aluminium rich. The number of strong acid sites is higher on the CoAPO-36 than on CoAPO-5, MAPO-5 and ZAPO-36. The catalytic activities of CoAPO-5, MAPO-5, ZAPO-36, CoAPO-36, MAPO-36 and MAPSO-36 in the 3-methylpentane and *o*-xylene conversion reactions were compared. The catalytic turnover rate per framework substituted atom in the conversion of *o*-xylene for CoAPO-36 is higher than for the MAPO-5, CoAPO-5, ZAPO-36 and MAPSO-36. In the ethylbenzene conversion reaction, the deactivation of the cobalt aluminophosphate and magnesium aluminophosphates of type 36 were studied.

Keywords: CoAPO-36; aluminophosphate molecular sieves; IR; XPS; binding energy; acidity; acid strength distribution and catalytic properties

1. Introduction

The aluminophosphate based molecular sieves comprising SAPO-*n*, MeAPO-*n*, MeAPSO-*n*, ElAPO-*n* and ElAPSO-*n* reported by the Union Carbide Corporation [1–4] have opened new vistas in catalytic fields. As such the aluminophosphate materials have neutral framework with no exchangeable cations. In the aluminophosphate materials, the negative framework charge or acidity can be generated by the isomorphous substitution of various divalent cations (Mg^{2+} , Mn^{2+} , Co^{2+} , Zn^{2+} , etc.) for trivalent aluminium cations or tetravalent cations (Si^{4+}) for pentavalent phosphorus cations. Flanigen et al. [1] have reported a series of novel crystalline microporous magnesium/cobalt/zinc/manganese incorporated aluminophosphates of type 36 molecular sieves. The type 36 aluminophosphate molecular sieves are of particular interest because of their higher catalytic activity among the other large and medium pore aluminophosphate molecular sieves [4–7]. The

type 36 aluminophosphate molecular sieve has a unique three-dimensional structure with monoclinic symmetry (cell parameters: $a = 13.148 \text{ \AA}$, $b = 21.577 \text{ \AA}$, $c = 5.164 \text{ \AA}$ and $\beta = 91.84^\circ$) and contains a unidimensional 12-ring elliptical channel system having a free aperture between 6.5 and 7.4 \AA [8,9]. The present work deals with the characteristics, surface properties, acidity, catalytic properties and deactivation behaviour of the CoAPO-36. Also, the catalytic properties of the cobalt/magnesium aluminophosphate of type 5 and zinc/magnesium/magnesium and silicon incorporated aluminophosphates of type 36 in the 3-methylpentane and *o*-xylene conversion reactions under identical experimental conditions were investigated.

2. Experimental

Preparation of CoAPO-36. The synthesis of the type 36 cobalt aluminophosphate molecular sieve was carried out using one gel composition and different synthesis conditions (table 1). Highly crystalline cobalt aluminophosphate of type 36 molecular sieve was synthesized by crystallizing a gel of composition: $2.0 n\text{-Pr}_3\text{N} \cdot 0.17\text{CoO} \cdot 0.92\text{Al}_2\text{O}_3 \cdot 1.01\text{P}_2\text{O}_5 \cdot 40\text{H}_2\text{O}$ hydrothermally in a teflon coated autoclave initially at 373 K for 96 h and finally at 423 K for 40 h. The crystals of $\text{Pr}_3\text{N-CoAPO-36}$ were thoroughly washed with deionized water, filtered, and dried in an air oven at 373 K for 16 h. The organic template (Pr_3N) was removed by calcination in the presence of air (flow rate $100 \text{ cm}^3 \text{ min}^{-1}$) at 763 K for 16 h. The sources of Al_2O_3 , P_2O_5 and CoO were pseudo-boehmite (Condea Chemie, FRG), ortho-phosphoric acid ((85%) Merck, FRG) and cobalt nitrate hexahydrate (Merck, FRG), respectively. The tri-*n*-propylamine used was synthetic grade

Table 1

Preparation of the type 36 cobalt aluminophosphate molecular sieve

Gel composition (molar): $2.0\text{Pr}_3\text{N} \cdot 0.17\text{CoO} \cdot 0.92\text{Al}_2\text{O}_3 \cdot 1.01\text{P}_2\text{O}_5 \cdot 40\text{H}_2\text{O}$

Synthesis conditions				Product phase(s)	Crystallinity (%)
initial		final			
temp. (K)	period (h)	temp. (K)	period (h)		
373	70	423	22	CoAPO-36 amph. (22%)	78
		423	40	CoAPO-36 amph. (20%)	80
		423	24	CoAPO-36 amph. (5%)	95
		423	40	CoAPO-36	100
373	96	423	40	COAPO-36	96

(Merck). The procedure for the gel preparation is similar to that of MAPO-36 reported earlier [10].

The molar compositions of the other aluminophosphate molecular sieves used in the present study are as follows: CoAPO-5 $0.176\text{CoO} \cdot 0.915\text{Al}_2\text{O}_3 \cdot 1.01\text{P}_2\text{O}_5$; MAPO-5 $0.156\text{MgO} \cdot 0.92\text{Al}_2\text{O}_3 \cdot 1.0\text{P}_2\text{O}_5$; ZAPO-36 $0.16\text{ZnO} \cdot 0.92\text{Al}_2\text{O}_3 \cdot 1.005\text{P}_2\text{O}_5$; MAPO-36 $0.16\text{MgO} \cdot 0.922\text{Al}_2\text{O}_3 \cdot 1.0\text{P}_2\text{O}_5$ and MAPSO-36 $0.158\text{MgO} \cdot 0.922\text{Al}_2\text{O}_3 \cdot 0.082\text{SiO}_2 \cdot 0.959\text{P}_2\text{O}_5$. The preparation, characterization, acidity and catalytic properties of ZAPO-36, MAPO-36 and MAPSO-36 are given elsewhere [5,7,10–12].

The details of the characterization techniques, acidity and catalytic activity measurements have already been reported [5,10,13,14]. The reaction conditions for the catalytic activity measurements are mentioned in the respective tables and figures.

3. Results and discussion

3.1. PREPARATION AND CHARACTERIZATION OF CoAPO-36

Table 1 shows the effect of the synthesis conditions on the product phase(s) and crystallinity of the cobalt aluminophosphate of type 36. In all the batches, the gel composition $[2.0n\text{-Pr}_3\text{N} \cdot 0.17\text{CoO} \cdot 0.92\text{Al}_2\text{O}_3 \cdot 1.01\text{P}_2\text{O}_5 \cdot 40\text{H}_2\text{O}]$ was the same, only the crystallization temperature and period were varied. By crystallizing the gel mixture at 423 K for 22 h and 40 h, the CoAPO-36 product was obtained with 77 and 80% purity. The phase purity increased to 95% by crystallizing the gel initially at 373 K for 70 h and further at 423 K for 24 h. Pure CoAPO-36 is obtained by crystallizing the gel initially at 373 K for 96 h and finally at 423 K for 40 h. It is observed that the initial crystallization of gel at 373 K for more than 96 h decreased the crystallinity of the product. Synthesis of phase free CoAPO-36 requires slightly higher concentration of the organic template (Pr_3N) as compared with the MAPO-36.

The characteristics of the cobalt-substituted aluminophosphate molecular sieve are presented in table 2. The elemental analysis of CoAPO-36 shows that there are

Table 2
Characteristics of the type 36 cobalt aluminophosphate molecular sieve

elemental composition	$[0.04\text{Co} \cdot 0.46\text{Al} \cdot 0.50\text{P}] \text{O}_2$
framework charge	$-0.04 \text{ electron/T atom}$
crystal shape	thin needle/rod-like
crystal length	14 μm
N_2 sorption capacity at 78 K	5.46 mmol g^{-1}
H_2O sorption capacity at 296 K	17.1 mmol g^{-1}
<i>n</i> -hexane sorption capacity at 296 K	1.48 mmol g^{-1}

no extraneous Al or P or Co elements present in the framework and Co substitutes for some of the Al in the aluminophosphate framework. CoAPO-36 crystals are thin needle/rod-like in shape and attached to a sphere (fig. 1). The N_2 , H_2O and *n*-hexane sorption capacity of CoAPO-36 is similar to those of MAPO-36 [10] and MAPSO-36 [7].

Figs. 2 and 3 show the TG/DTG/DTA curves for the decomposition of $\text{Pr}_3\text{N-CoAPO-36}$ in an inert ((nitrogen) (A)) and in an oxidizing ((air) (B)) atmosphere.

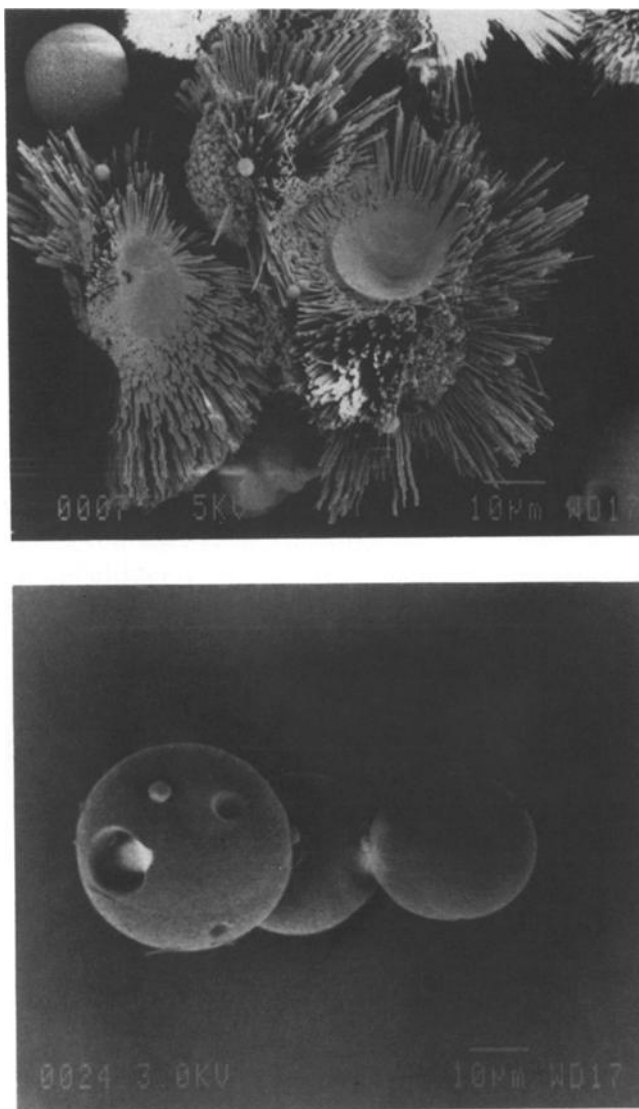


Fig. 1. Scanning electron photomicrographs of $\text{Pr}_3\text{N-CoAPO-36}$.

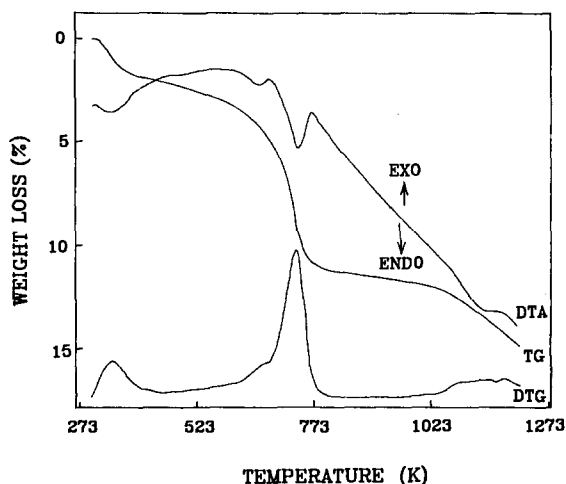


Fig. 2. TG, DTG and DTA curves for the decomposition of $\text{Pr}_3\text{N-CoAPO-36}$ in nitrogen.

The thermal analysis data of $\text{Pr}_3\text{N-CoAPO-36}$ is presented in table 3. The results of thermal analysis indicate that in an inert atmosphere all the processes occurring in the removal of occluded materials from the cobalt aluminophosphate are endothermic. The total weight loss amounts to 14.2 wt% in inert atmosphere. In the first stage, the weight loss of 2.9 wt% at 303–570 K is due to the desorption of physisorbed water and tri-*n*-propylamine from the cobalt aluminophosphate. The major weight loss (8.0 wt%) occurs in the second stage at 570–811 K. The second stage corresponds to the desorption of tri-*n*-propylamine and possibly to cracking of the occluded tri-*n*-propylamine molecules to smaller molecules. In the third stage (811–1203 K), the weight loss of 3.3 wt% is mostly due to the very slow de-

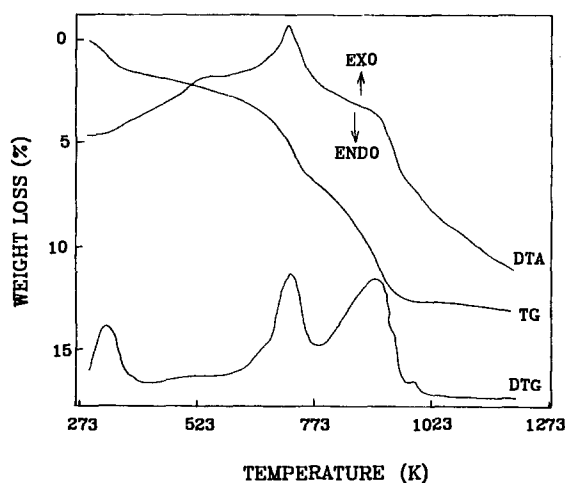


Fig. 3. TG, DTG and DTA curves for the decomposition of $\text{Pr}_3\text{N-CoAPO-36}$ in air.

Table 3

TG, DTG and DTA data of the as-synthesized cobalt aluminophosphate of type 36 molecular sieve

Decomp. zone	Temp. range (K)	Wt. loss (%)	Total wt. loss (%)	Peak temp. (K)	
				DTG	DTA
<i>nitrogen</i>					
I	303–570	2.9	2.9	345	338 ^a
II	570–811	8.0	10.9	730	649 ^a , 734 ^a
III	811–1203	3.3	14.2	1123	1163 ^a
<i>air</i>					
I	303–558	2.8	2.8	338	352 ^a
II	558–751	4.2	7.0	725	556 ^b , 723 ^b
III	751–972	6.9	13.9	909	913 ^b
IV	972–1203	0.5	14.4	982	980 ^b

^a Endothermic.^b Exothermic.

sorption of ammonia and/or tri-*n*-propylamine adsorbed strongly on the high energy sites of CoAPO-36. In an oxidizing atmosphere, the thermal analysis results indicate that the decomposition in the presence of air is a complex process which occurs in four distinct stages with a total weight loss of 14.4 wt%. In the first stage, the desorption of physisorbed water and tri-*n*-propylamine from Pr₃N-CoAPO-36 occurs at the 303–558 K temperature range and the weight loss is 2.8 wt%. In the second and third stages, a major weight loss occurs at 558–751 and 751–972 K, respectively. The fourth weight loss (0.5 wt%) occurs at 972–1203 K. In these stages, the removal of tri-*n*-propylamine is expected to be due mostly to its oxidative decomposition, which is an exothermic process.

The bulk and surface composition of the as-synthesized CoAPO-36 and the calcined CoAPO-36 samples are presented in table 4. The surface concentrations of the elements on the as-synthesized and the calcined cobalt aluminophosphate of type 36 are as follows: Pr₃N-CoAPO-36: C_{1s} 26.1%; N_{1s} 1.2%; Co_{2p_{3/2}} 0.9%; Al_{2p}

Table 4

Bulk and surface composition of the as-synthesized and calcined cobalt aluminophosphate of type 36 molecular sieve

Sample	Atomic ratio ^a					
	Al/P		Co/P		[(Co + Al)/P]	
	B	S	B	S	B	S
Pr ₃ N-CoAPO-36	0.91	1.03	0.08	0.07	0.99	1.11
CoAPO-36	0.91	0.99	0.08	0.06	0.99	1.05

^a B, bulk; S, surface.

12.1%; P_{2p} 11.8%; O_{1s} 48.0% and calcined CoAPO-36: Co_{2p_{3/2}} 1.1%; Al_{2p} 16.8%; P_{2p} 17.0%; O_{1s} 65.1%. In the uncalcined and calcined CoAPO-36 samples, the Al/P ratio on the surface is higher than in the bulk, which indicates that the concentration of aluminium is higher on the surface. Comparisons of bulk and surface Co/P ratios for Pr₃N-CoAPO-36 and CoAPO-36 indicate that the surface concentration of Co is lower than in the bulk.

Table 5 shows the XPS binding energy data for Pr₃N-CoAPO-36. The main carbon signals observed on CoAPO-36 sample did not result from the adventitious contamination but from the organic template (tri-*n*-propylamine). The binding energies measured for Co_{2p_{3/2}} and Co_{2p_{1/2}} in Pr₃N-CoAPO-36 are 782.2 and 796.5 eV, respectively. The observed binding energies of Al_{2p}, P_{2p} and O_{1s} are close to that of Al_{2p}, P_{2p} and O_{1s} in MAPO-36 [10] and ZAPO-36 [11].

3.2. ACIDITY

Fig. 4 shows the infrared spectrum after the desorption of pyridine at 473 K from CoAPO-36 pretreated at 753 K in vacuum. The bands at 1449 and 1544 cm⁻¹ are ascribed to Lewis and Brønsted acid sites [15], respectively, indicating the presence of Brønsted and Lewis acid sites on CoAPO-36 material. In the cobalt aluminophosphate, the framework acidity is produced by the substitution of Co into some of the Al sites in the AlPO₄-framework.

The temperature programmed desorption of pyridine chromatograms on the cobalt aluminophosphate at different initial sorbate (pyridine) loadings presented in fig. 5 indicated the presence of two types of acid site on CoAPO-36. The peak maximum temperature (T_m) (of the first peak) for the desorption is shifted toward the higher temperature side with the decrease in the value of θ_1 (up to 0.02 mmol g⁻¹), which indicates the presence of acid strength distribution on the cobalt aluminophosphate.

Fig. 6A shows the temperature dependence of the chemisorption of pyridine on the CoAPO-36 obtained from the STD data. The chemisorption capacity of pyridine at higher temperatures points to the involvement of the stronger sites. The acid strength distribution on the cobalt aluminophosphate is shown in fig. 6B. The columns in fig. 6B show the distribution of the sites involved in the chemisorption/desorption of pyridine. Each column of the acid strength distribution represents the number of sites measured in terms of pyridine desorbed in the corresponding tem-

Table 5
XPS data for the as-synthesized cobalt aluminophosphate of type 36 molecular sieve

Binding energy (eV) ^a					
N _{1s}	Co _{2p_{3/2}}	Co _{2p_{1/2}}	Al _{2p}	P _{2p}	O _{1s}
400.4	782.2	796.5	74.2	133.7	531.4

^a Referenced to C_{1s} = 284.4 eV.

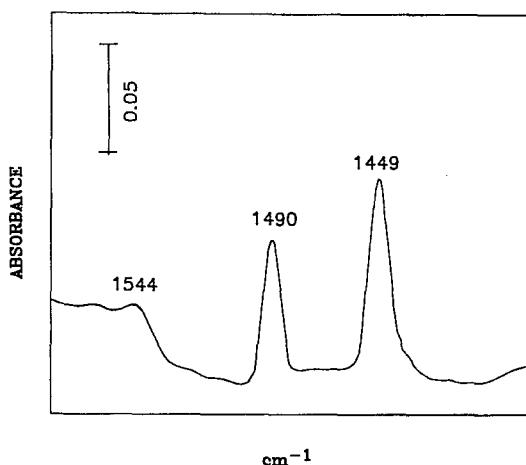


Fig. 4. In situ infrared spectrum of chemisorbed pyridine on CoAPO-36 (pyridine chemisorbed at 473 K).

perature step. The strength of these sites is expressed in terms of the desorption temperature of pyridine, T_d , which lies in the range in which chemisorbed pyridine is desorbed. The decrease in the chemisorption of pyridine with increase in the temperature for the CoAPO-36 (fig. 6A) revealed that the pyridine chemisorption sites on the aluminophosphate are not of equal strength, thus indicating the presence of acid strength distribution on the material. The temperature programmed desorption and the stepwise thermal desorption of pyridine investigations have shown the presence of a broad acid strength distribution on the cobalt aluminophosphate. The amount of the base (pyridine) chemisorbed over the HY, HKL, HM, H-ZSM-5, H-ZSM-8 and H-ZSM-11 zeolites [16] at 623 K was 0.78, 0.22, 0.77, 0.25, 0.31, and 0.07 mmol g⁻¹, respectively. The amount of the base chemisorbed (at 623 K) on the low and high silica zeolites is higher than on the aluminophosphate

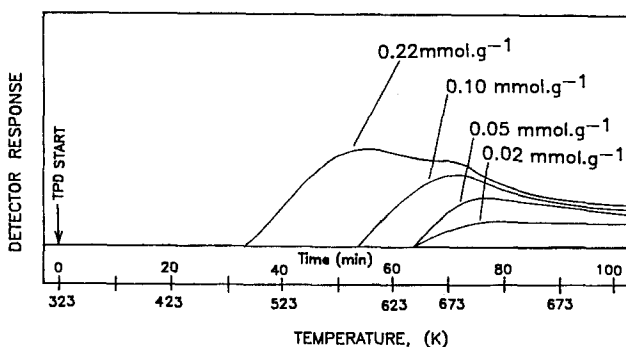


Fig. 5. TPD chromatograms of pyridine on CoAPO-36 (amount of catalyst: 0.23 g; He flow rate, 10 cm³ min⁻¹; heating rate, 5 K min⁻¹).

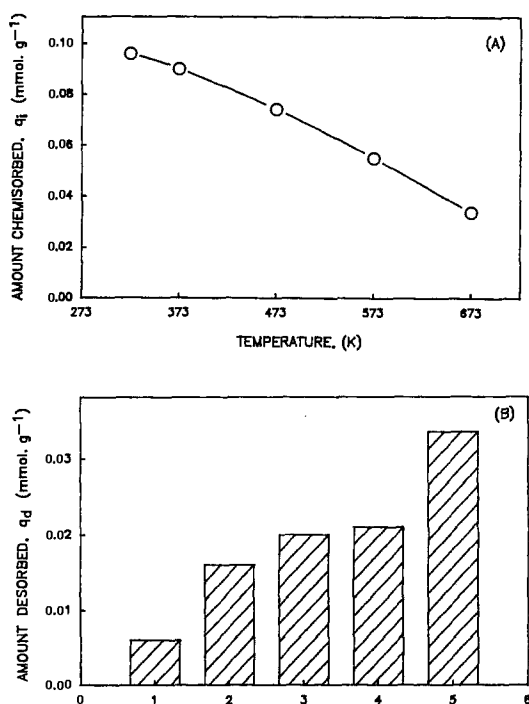


Fig. 6. (A) Temperature dependence of the chemisorption of pyridine on CoAPO-36. (B) Site energy distribution on CoAPO-36.

materials. The number of strong acid sites, expressed in terms of the pyridine chemisorbed and Brønsted and Lewis acid site ratios over the different aluminophosphates are given in table 6. The amount of pyridine chemisorbed above 623 K over

Table 6

Comparison of the acidity and catalytic turnover rates for the different element substituted aluminophosphates

	CoAPO-36	CoAPO-5	MAPO-5	MAPO-36	ZAPO-36	MAPSO-36
mmol E/g ^a	0.646	0.705	0.644	0.661	0.643	Mg 0.655 Si 0.340
strong acid sites above 623 K	0.052	0.011	0.017	0.057	0.045	0.064
Brønsted/Lewis acid sites ratio at 473 K	0.28	0.23	0.24	0.29	0.264	0.31
catalytic activity ^b	8.65	3.9	7.2	10.2	7.8	7.0

^a E, framework substituted element (i.e. Co in CoAPO-5/CoAPO-36, Mg in MAPO-5/MAPO-36, Zn in ZAPO-36, (Mg and Si) in MAPSO-36).

^b Turnover rate; expressed in terms of the number of moles reacted per framework substituted atom(s) per second.

CoAPO-36 is higher than that of ZAPO-36 [11] and lower than those of MAPO-36 [10] and MAPSO-36 [7]. Comparison of CoAPO-36, MAPO-5 and CoAPO-5 for their acidity indicated that the amount of pyridine chemisorbed above 673 K was lower on CoAPO-5 and MAPO-5. The order of the number of strong acid sites on these materials is as follows: CoAPO-5 < MAPO-5 << ZAPO-36 < CoAPO-36 < MAPO-36 < MAPSO-36. Differences in the number of strong acid sites on CoAPO-36, ZAPO-36 and MAPO-36 are related to the nature of the framework substituted metal, since all the materials have the same structure and similar concentration of framework substituted metal. This indicates that the incorporation of cobalt in the AlPO₄-36 framework produces a lower number of strong acid sites than the incorporation of magnesium or a higher number of strong acid sites than the incorporation of zinc.

3.3. CATALYTIC PROPERTIES

In table 7, the results of 3-methylpentane conversion over CoAPO-36 are compared to similar results obtained with MAPO-5, CoAPO-5, ZAPO-36, MAPO-36 and MAPSO-36. In the 3-methylpentane conversion reaction, CoAPO-36 showed higher conversion and concentration of aromatics formation as compared with

Table 7

Data on the conversion of 3-methylpentane on ZAPO-36, CoAPO-36, MAPO-36, MAPSO-36, CoAPO-5 and MAPO-5^a

Catalyst	ZAPO-36 ^b	CoAPO-36	MAPO-36	MAPSO-36	CoAPO-5	MAPO-5
conversion (%)	16.1	21.2	31.9	46.0	1.6	2.2
aromatics conc. (wt%)	1.7	2.2	3.5	5.2	0.2	0.4
<i>product distribution (hydrocarbon (wt%))</i>						
CH ₄	4.3	2.8	1.6	2.0	2.7	4.5
C ₂ -aliphatics	25.5	26.0	24.5	24.8	18.8	31.8
C ₃ -aliphatics	25.1	23.7	26.6	28.7	18.0	13.6
C ₄ -aliphatics	27.0	21.9	12.2	22.8	19.6	14
C ₅₊ -aliphatics	7.5	15.8	24.1	10.4	25.0	18
aromatics	10.6	10.2	11.0	11.3	12.5	18.1
total	100	100	100	100	100	100
<i>aromatics distribution (wt%)</i>						
benzene	1.1	11.6	11.4	8.3		
toluene	16.5	22.2	17.1	25.8		
xylene	35.4	11.0	34.3	17.8		
trimethyl benzenes	23.5	33.0	20.1	10.2		
other C ₉₊ -aromatics	23.5	22.2	17.1	37.9		
total	100	100	100	100		

^a Reaction conditions: weight of catalyst 0.045 g, He flow rate 110 cm³ min⁻¹, pulse size 5 µl, temperature 673 K.

^b Ref. [11].

CoAPO-5, MAPO-5 and ZAPO-36 but lower than that of MAPO-36 and MAPSO-36. The higher catalytic activity exhibited by the CoAPO-36 than CoAPO-5 and ZAPO-36 is consistent with the presence of stronger acid sites and the higher Brønsted to Lewis acid sites ratio (table 6). The observed order of catalytic activity and aromatics selectivity is the same as the order found for strong acid sites, namely MAPSO-36 > MAPO-36 > CoAPO-36 > ZAPO-36 > MAPO-5 > CoAPO-5. Our earlier investigations [7,10,11] on the temperature programmed desorption and the stepwise thermal desorption of pyridine over these materials showed that the amounts of pyridine chemisorbed on MAPSO-36 and MAPO-36 above 673 K were significantly higher than on CoAPO-5, ZAPO-36 and CoAPO-36, indicating the presence of stronger acidic sites. The aliphatics distribution in the 3-methylpentane conversion reaction is quite different among the catalysts. CoAPO-36 showed higher C₂- and C₅₊-aliphatics and lower C₃- and C₄-aliphatics formation as compared to ZAPO-36 and MAPSO-36. The distribution of the aromatics formed on ZAPO-36, CoAPO-36, MAPO-36 and MAPSO-36 is quite different. CoAPO-36 shows higher benzene and toluene formation than ZAPO-36 and MAPO-36. Also, the formation of trimethylbenzenes was higher over CoAPO-36.

Table 8 shows the conversion of cyclohexane, cycloheptane and cyclooctane over the cobalt aluminophosphate of type 36. In these reactions, CoAPO-36 shows

Table 8

Data on the conversion of cyclohexane, cycloheptane and cyclooctane on the type 36 cobalt aluminophosphate molecular sieve ^a

Reactant	Cyclohexane	Cycloheptane	Cyclooctane
conversion (%)	17.5	34.2	38.0
aromatics conc. (wt%)	3.7	9.0	13.4
<i>product distribution (hydrocarbon (wt%))</i>			
CH ₄	1.1	1.1	0.8
C ₂ -aliphatics	9.7	7.9	6.0
C ₃ -aliphatics	12.6	12.3	10.0
C ₄ -aliphatics	12.1	12.0	10.0
C ₅₊ -aliphatics	43.4	40.4	37.9
aromatics	21.1	26.3	35.3
total	100	100	100
<i>aromatics distribution (wt%)</i>			
benzene	1.6	1.8	0.7
toluene	19.4	19.3	14.2
ethylbenzene	5.9	8.9	6.7
xylenes	39.5	37.8	44.8
trimethyl benzenes	27.0	18.9	22.4
other C ₉₊ -aromatics	6.6	13.3	11.2
total	100	100	100

^a Reaction conditions: weight of catalyst 0.045 g, He flow rate 110 cm³ min⁻¹, pulse size 5 µl, temperature 673 K.

significant activity and aromatics formation. In the cyclohexane, cycloheptane and cyclooctane conversion reactions, it is observed that the conversion and aromatics formation increases with the increase in the number of carbon atoms in the cycloalkane ring. The aliphatic distributions in these reactions are less affected. Also the formation of C₁- to C₅₊-aliphatics and toluene decreases with the number of carbon atoms in the cycloalkane ring. In the 3-methylpentane and cyclohexane conversion, the catalytic activity of CoAPO-36 decreased significantly after poisoning the strong acid sites by pyridine (at 673 K). The conversions of 3-methylpentane and cyclohexane on the pyridine poisoned CoAPO-36 were 2.6 and 2.1 wt%, respectively.

CoAPO-36 showed higher catalytic activity in *o*-xylene conversion reaction (table 9) than CoAPO-5 and ZAPO-36. The xylene loss (which reflects the selectivity for isomerization in the *o*-xylene conversion) is lowest and the selectivity for *p*- and *m*-xylenes was highest for CoAPO-36 as compared with ZAPO-36, MAPO-36 and MAPSO-36. The disproportionation is more pronounced than the isomerization in *o*-xylene conversion reaction over MAPO-36 and MAPSO-36. In table 6, the catalytic activities of the aluminophosphates in the *o*-xylene conversion reaction are expressed in terms of the catalytic turnover rate per framework substituted atom (N_E) (i.e. Co in CoAPO-36 and CoAPO-5, Mg in MAPO-5/MAPO-36, Zn in ZAPO-36 and (Mg + Si) in MAPSO-36). The turnover rate per framework substituted atom (N_E) for CoAPO-36 is higher than for CoAPO-5, MAPO-5, ZAPO-

Table 9

Data on the *o*-xylene conversion on ZAPO-36, CoAPO-36, MAPO-36, MAPSO-36, CoAPO-5 and MAPO-5^a

Catalyst	ZAPO-36	CoAPO-36	MAPO-36	MAPSO-36	CoAPO-5	MAPO-5
conversion (%)	45.2	50.4	60.5	63.5	25.0	42.0
<i>product distribution (hydrocarbon (wt%))</i>						
aliphatics	0.2	0.2	0.4	0.5	0.3	0.4
benzene	0.3	0.2	0.5	0.4	0.4	0.4
toluene	2.6	2.0	5.9	6.3	1.5	2.2
<i>p</i> -xylene	16.5	19.4	19.6	17.9	8.9	14.7
<i>m</i> -xylene	21.0	25.0	25.1	24.1	10.7	20.7
<i>o</i> -xylene	54.8	49.3	39.5	36.5	75.0	58.0
trimethylbenzenes	3.8	2.5	7.8	12.9	2.2	3.0
other C ₉₊ -aromatics	0.8	1.4	1.2	1.5	1.0	0.6
total	100	100	100	100	100	100
xylene loss (wt%)	7.7	6.3	15.8	21.5	5.4	6.6
selectivity for <i>p</i> - and <i>m</i> -xylene (%)	83.0	87.0	74.0	66.0	78.4	85.5
<i>p</i> -X/ <i>m</i> -X	0.79	0.78	0.78	0.74	0.83	0.71

^a Reaction conditions: weight of catalyst 0.045 g, He flow rate 115 cm³ min⁻¹, pulse size 5 µl, temperature 673 K.

36 and MAPSO-36 and the order of N_E is as follows: CoAPO-5 < MAPSO-36 < MAPO-5 < ZAPO-36 < CoAPO-36 < MAPO-36.

The results on the conversion of toluene, ethylbenzene, propylbenzene and butylbenzene on the type 36 cobalt aluminophosphate are presented in table 10. CoAPO-36 shows significant activity in these reactions. Fig. 7 shows the results of ethylbenzene conversion on CoAPO-36 and MAPO-36 at 673 K. The conversion of ethylbenzene (in the first pulse experiment) on CoAPO-36 is lower than that on MAPO-36. Influence of pulse number on the fractional ethylbenzene activity (x) (where, $x = (\text{conversion of ethylbenzene for a particular pulse})/(\text{conversion of ethylbenzene for the first pulse})$) of CoAPO-36 and MAPO-36 shown in fig. 7 represents the deactivation trends. The deactivation of CoAPO-36 is more pronounced than that of MAPO-36. The conversion of toluene on the fresh CoAPO-36 was 44% and after the injection of the 30th pulse of ethylbenzene, the observed toluene conversion was 23%. The deactivated cobalt aluminophosphate was regenerated at 773 K in the flow of a mixture of helium and oxygen (20% O for 5 h). Regenerated CoAPO-36 showed regained in its catalytic activity by 92%.

4. Conclusions

Pure CoAPO-36 can be prepared by hydrothermal crystallization of a gel of composition: $2.0n\text{-Pr}_3\text{N}\cdot 0.17\text{CoO}\cdot 0.92\text{Al}_2\text{O}_3\cdot 1.01\text{P}_2\text{O}_5\cdot 40\text{H}_2\text{O}$ initially at 373 K for 96 h and finally at 423 K for 40 h. CoAPO-36 possesses higher acidity than CoAPO-5, MAPO-5 and ZAPO-36, but lower than MAPO-36 and MAPSO-36. CoAPO-36 shows significant catalytic activity in the conversion of aliphatic and

Table 10

Data on the conversions of toluene, ethylbenzene, propylbenzene and butylbenzene on the type 36 cobalt aluminophosphate molecular sieve ^a

Reactant	Toluene	Ethylbenzene	Propylbenzene	Butylbenzene
conversion (%)	44.0	76.2	95.0	100
<i>product distribution (hydrocarbon (wt%))</i>				
aliphatics	0.5	19.5	26.7	37.4
benzene	18.8	42.2	45.2	46.5
toluene	56.0	6.2	7.6	5.6
ethylbenzene	—	23.8	—	—
propylbenzene	—	—	5.0	—
xylene	20.4	0.2	4.5	1.8
trimethylbenzenes	3.5	2.1	3.3	0.8
other C ₉₊ -aromatics	0.8	6.0	7.7	7.9
total	100	100	100	100

^a Reaction conditions: weight of catalyst 0.1 g, He flow rate 30 cm³ min⁻¹, pulse size 5 μ l, temperature 673 K.

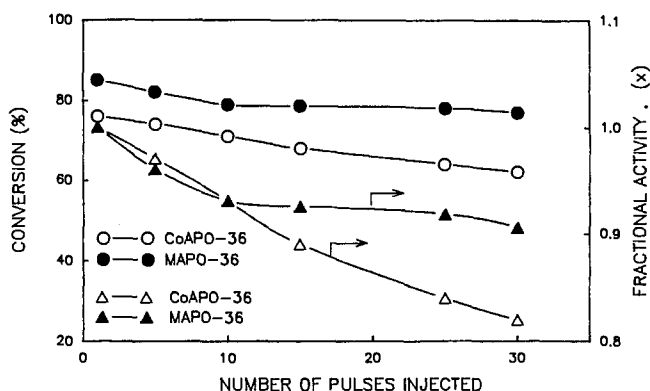


Fig. 7. Effect of the pulse number on the cumene cracking conversion and fractional cumene cracking activity on CoAPO-36 and MAPO-36 (reaction conditions: amount of catalyst 0.045 g, He flow rate $100 \text{ cm}^3 \text{ min}^{-1}$, temperature 673 K, pulse size $5 \mu\text{l}$).

aromatic hydrocarbons. In the conversions of 3-methylpentane and *o*-xylene, CoAPO-36 exhibits higher catalytic activity as compared with MAPO-5, CoAPO-5 and ZAPO-36.

Acknowledgement

The author is grateful to the Alexander von Humboldt Foundation, Bonn, Germany for an award of an international research fellowship.

References

- [1] E.M. Flanigen, B.M. Lok, R.L. Patton and S.T. Wilson, *Pure Appl. Chem.* 58 (1986) 1351.
- [2] E.M. Flanigen, B.M. Lok, R.L. Patton and S.T. Wilson, *Proc. 7th Int. Zeolite Conf.* (Kodansha/Elsevier, Tokyo/Amsterdam, 1986) p. 103.
- [3] E.M. Flanigen, R.L. Patton and S.T. Wilson, *Stud. Surf. Sci. Catal.* 37 (1988) 13.
- [4] S.T. Wilson and E.M. Flanigen, *ACS Symp. Ser.* 398 (1989) 329.
- [5] D.B. Akolekar, *J. Catal.* 144 (1993) 148.
- [6] D.B. Akolekar and S. Kaliaguine, *J. Chem. Soc. Faraday Trans.* 89 (1993) 4141.
- [7] D.B. Akolekar, *Zeolites* 14 (1994) 53.
- [8] J.V. Smith, J.J. Pluth and K.J. Andries, *Atlas of Zeolite Structure Types*, 3rd rev. Ed., eds. W.M. Meir and D.H. Olson (Butterworth-Heinemann, London, 1992) p. 50.
- [9] J.V. Smith, J.J. Pluth and K.J. Andries, *Zeolites* 13 (1993) 166.
- [10] D.B. Akolekar, *J. Catal.* 143 (1993) 148.
- [11] D.B. Akolekar, *Zeolites*, submitted.
- [12] D.B. Akolekar, *Appl. Catal.* (1994), in press.
- [13] V.S. Nayak and V.R. Choudhary, *Appl. Catal.* 4 (1982) 333.
- [14] V.S. Nayak and V.R. Choudhary, *J. Catal.* 81 (1983) 26.
- [15] J.W. Ward, in: *Zeolite Chemistry and Catalysis*, ACS Monograph No. 171, ed. J.A. Rabo (Am. Chem. Soc., Washington, 1976) p. 118.
- [16] V.R. Choudhary and D.B. Akolekar, *J. Catal.* 119 (1989) 525.